

Statistical field theory of the transmission of nerve impulses

Gianluigi Zangari del Balzo (✉ gianluigi.zangaridelbalzo@gmail.com)

Research

Keywords: action potentials, ion channels, Hodgkin-Huxley model, Ising model, statistical field theory, quasi particles, Multiple Sclerosis, particle physics, complex networks.

Posted Date: November 3rd, 2020

DOI: <https://doi.org/10.21203/rs.3.rs-16896/v3>

License:  This work is licensed under a Creative Commons Attribution 4.0 International License.

[Read Full License](#)

Version of Record: A version of this preprint was published on January 6th, 2021. See the published version at <https://doi.org/10.1186/s12976-020-00132-9>.

Statistical field theory of the transmission of nerve impulses

Gianluigi Zangari del Balzo

Correspondence: gianluigi.zangaridelbalzo@gmail.com

Abstract

Background

Stochastic processes leading voltage-gated ion channel dynamics on the nerve cell membrane are a sufficient condition to describe membrane conductance through statistical mechanics of disordered and complex systems.

Results

Voltage-gated ion channels in the nerve cell membrane are described by the Ising model. Stochastic circuitual elements called "Ising machines" are introduced. Action potentials are described as quasi-particles of a statistical field theory for the Ising system.

Conclusions

The particle description of action potentials is a new powerful tool to describe the generation and propagation of nerve impulses. We thus have the opportunity to exploit another useful point of view to describe the generation and propagation of nerve impulses, especially when classical electrophysiological models break down.

Moreover, the particle description allows us to develop new hardware and software devices based on general and theoretical physics to study neurodegenerative and demyelinating diseases as Multiple Sclerosis and Alzheimer's disease, even integrated by connectomes. It is also suitable for the study of complex networks, quantum computing, artificial intelligence, machine and deep learning, cryptography, ultra-fast lines for entanglement experiments and many other applications of medical, physical and engineering interest.

Keywords

action potentials, ion channels, Hodgkin-Huxley model, Ising model, statistical field theory, quasi particles, Multiple Sclerosis, particle physics, complex networks.

Background

In 1952 British physiologists Sir Alan Lloyd Hodgkin (1914-1998) and Sir Andrew Fielding Huxley (1917-2012) at the University of Cambridge demonstrated the existence of selective and voltage-dependent ion channels in the nerve cell membrane with five famous pioneers works published in the Journal of Physiology. They received the Nobel Prize for Medicine in 1963 together with the Australian physiologist Sir John Carew Eccles (1903-1997) [1, 2, 3, 4, 5]. Nowadays, after almost 68 years, the success and evolution of the Hodgkin and Huxley models, hereinafter referred to simply as "HH models", are still alive and continuously stimulate the development of new topics and branches of physiology and neurosciences [5, 6, 7, 8]. In 1976, the "Patch Clamp" method, developed by Erwin Neher and Bert Sakmann [9], who received the Nobel Prize in Medicine in 1991, demonstrated among other things:

1. Microcurrents. The existence of microscopic electric currents of intensity in the order

of pA (picoampere) that flow through each ion channel, transporting on average thousands of ions per millisecond (Fig. 1);

2. Stochastic channels. The stochastic dynamics of opening/closing (“gating”) of each ion channel.

Methods

The recording of current flow through individual channels (Fig. 1), shows stochastic fluctuations between closed and open states. This is a sufficient condition to define the concept of membrane conductance through statistical mechanics of disordered and complex systems [10, 11, 12, 13, 14, 15]. We will therefore start from the basic formalism developed by Hodgkin and Huxley to describe the processes carried out by the conductances of the Na⁺ and K⁺ channels to explain the generation of action potentials. The opening and closing of voltage-gated ion channels (“gating”) is a physical process that involves complex conformational changes in the structure of each channel, or in the sub-units of which it is composed. Opening a gate is generally called “conductance activation”, while closing “conductance deactivation” [5, 6, 7, 8].

The Ising model

We define gating using a binary stereotyped form as an Ising spin variable. We will therefore consider a distribution of N voltage-dependent ion channels on an elementary region (slice) of a nerve membrane (axon) made by a thin ring of radius $\rho \sim 10\mu\text{m}$ and thickness $h \sim 1\text{nm}$. (See Fig. 2). A population of N ion channels of a certain superfamily (Na⁺, K⁺, Cl⁻, ..) will be distributed on an axon section made by a thin ring (represented in figure 2 and topologically modeled in fig. 3), formally described by the Hamiltonian of the one- dimensional Ising Model for each superfamily of channels:

$$H_I = -J \sum_{i=1}^N S_i S_{i+1} - \phi \sum_{i=1}^N S_i \quad (1)$$

The border condition (See Fig. 3) is $S_{N+1} = S_1$, where S_i are N Ising variables ($S_i = +1$ corresponds to an open channel state, while $S_i = -1$ corresponds to a closed channel state, for $i= 1, \dots, N$). The energy of interaction between the channels of the same superfamily is represented by the variable $J > 0$, which we assume isotropic and “ferromagnetic”, while ϕ (mV) is the electrochemical driving force, hereinafter called “driving force” $\phi = V - E_\gamma$ where V (mV) is the membrane potential and E_γ (mV) is the equilibrium potential of each superfamily of ion channels.

The Helmholtz Free Energy will be [13]

$$A_I(\phi, \beta) = -NJ - \frac{N}{\beta} \log \left[\cosh(\beta\phi) + \sqrt{\sinh^2(\beta\phi) + e^{-4\beta J}} \right] \quad (2)$$

And the magnetization will be

$$M_I(\phi, \beta) = \langle \sum_{i=1}^N S_i \rangle = -\frac{\partial}{\partial \phi} [A_I(\phi, \beta)] = \frac{N \sinh(\beta \phi)}{\sqrt{\sinh^2(\beta \phi) + e^{-4\beta J}}} \quad (3)$$

Where $\beta = \frac{1}{k_B T}$; k_B is the Boltzmann constant and T the absolute temperature. We will see shortly what the observables of the Ising model mean in our case, above all the magnetization, which will be our main observable. Before that it is necessary to discuss a formal issue about the relationship between our stochastic model and the Hodgkin-Huxley model, which will help us to explain our choices.

Ising and Hodgkin-Huxley

The sigmoid distribution of spin magnetization reproduced in figure 4 recalls the activation and inactivation limit functions n_∞ , m_∞ , h_∞ defined by the HH models (Fig. 5) and the conductances in function of the membrane potential for the Na^+ and K^+ channels (Fig 6). The sigmoid characteristic is typical of a cooperative process, as in the present case. However, in the HH model, the limit function for the conductance is

$$n_\infty(\phi) = \frac{\alpha_n(\phi)}{\alpha_n(\phi) + \beta_n(\phi)} \quad (4)$$

expressed by the gating fractions $\alpha_n(V)$ and $\beta_n(V)$ as a function of the potential [5, 7, 8] The gating fractions are defined on the basis of general thermodynamic considerations (Boltzmann) [5, 7, 8]

$$n_\infty(V) = \frac{1}{1 + \left(\frac{A_2}{A_1}\right) \exp\left(\frac{(B_1 - B_2)\phi}{\phi_T}\right)} \quad (5)$$

In the present case, the choice of the one-dimensional Ising model obeys a different methodological choice that we use to call “congruence” because it wants to express a stronger link between the physics of gating process and its mathematical law in a closed form, that is without using a “metatheory”. Indeed, when we look for a law of nature, we try, among others, a phenomenological law, that is, we resort to a metatheory. In this case, to fit the experimental case, an element or a formal expression of a metatheory - for example a mathematical model - must necessarily depend on a set of parameters that will have to be fine-tuned manually to fit the experimental data, as in the case of the HH model. Therefore, to interpolate the experimental data (Fig. 6), we discard function (5) of the HH model because it is a “metatheory”, but we choose the one-dimensional Ising model because it presents the congruence in closed form we are looking for¹.

¹ The concept of *congruence* was used by the present author in the context of the unconventional statistical calculus system called “SHT”, based on the theory of categories and intended for the study of complex and disordered systems (derived and patented between 1997 and 2011 [16]). From a practical point of view, the SHT calculus does not “destructively interfere” with the sample, but analyzes the system *sic rebus stantibus*, considering also the “junk”, the environmental background and the noise. SHT treats the sample as a “dynamic system”. It studies maps and transforms, looks for critical points and transitions, bifurcations and attractors. For example, if SHT finds an attractor, it will become a “category” of the experiment. This is precisely our meaning of “congruence”. From a statistical point of view, a congruent model is a probability

Results

The Ising conductance

Recall the expression (3) for the magnetization in the one-dimensional Ising model. According to our methodological constraint, here the magnetization becomes the conductance of the nerve membrane.

We thus define the “Ising conductance” g_I as the magnetization:

$$g_I := M_I = \langle \sum_{i=1}^N S_i \rangle \quad (6)$$

In practice, we will consider the specific conductance (mSiemens / cm^2) so that the membrane current per unit area will be expressed by Ohm’s Law

$$i_m = g_I(V - E_\gamma) \quad (7)$$

Where V (mV) is the membrane potential and E_γ (mV) is the equilibrium potential of each superfamily of channels.

From our model we define a stochastic circuit element which we call for convenience of reading “Ising Neural Machine” (INM), briefly “Ising Machine”, and we indicate it with a rhomboid frame icon². We place the INMs in the equivalent circuit with single compartment of figure 7 defined for two superfamilies of ion channels (Na^+ and K^+). Now we want to discuss the problem of the generation of action potentials. In the following we will for brevity refer to action potentials as spikes .

Nuons

With reference to Fig. 8 [6], which shows the reconstruction of an action potential after Hodgkin and Huxley, 1952d [4, 6], we find that an increase in the conductance of the Na^+ channels triggers a spike. A flow of Na^+ ions enters the nerve cell, causing the membrane potential to depolarize up to the E_{Na} value. The depolarization activates the (delayed) conductance of the K^+ channels which provokes the escape of K^+ ions from the nerve cell, thus blocking the Na^+ channels and repolarizing the membrane up to the

density. Any metatheory is not a category of the experiment. In the case of very large and complex systems, the analysis is generally carried out on many logical levels (see for example some works on complex systems and particle physics [17, 18]). In other cases, the analysis is conducted by arranging the data on an REM energy landscape and studying the configurations of minimum entropy [19].

² As a functional icon synonymous of complexity, we chose the “complex” polyhedron called Icosi-icosahedron first described by Edmund Hess in 1876. It is the result from the auto dual composition of 10 tetrahedra enclosing a dodecahedron, all intersected by an icosahedron. The compound of ten tetrahedra is one of the five regular polyhedral compounds. This polyhedron can be seen as either a stellation of the icosahedron or a compound. The vertices correspond to the pairs 2 {5,3} [10 {3,3}] 2 {3,5}. After “Polytopes and their Incident Matrices”, courtesy of Richard Klitzing [20, 21].

E_K value (“refractory period”). Since K^+ conductance becomes transiently higher than its rest value, the membrane potential exceeds its negative rest value (“hyperpolarization”), so that both the K^+ conductance and the (possibly) residual Na^+ conductance are inactivated. Finally, the membrane returns to its resting value and it is ready to trigger a new spike.

With reference to the next Fig. 9, the local depolarization of the nerve membrane is started by a current of carriers (a synaptic potential, an artificial stimulus, or a passive current) which triggers a spike (see Figures 9a and 9d). From our point of view, consider for a certain instant $t > 0$ a single carrier triggering a pair of “Ising machines” (Na^+/K^+) housed into an annular section of the nerve cell membrane (See Figures 2, 9b and 9e). As it will be clarified below, only one annular section is activated at a time $t > 0$.

At this point, we remind that the activation of the voltage-dependent ion channels involves reversible conformational changes in the membrane of the nerve cell (gating) which configure a structural deformation of the membrane itself. The deformation tends to chase the carrier and to propagate along the nerve axis in the direction of the carrier itself, activating one annular section at a time. The refractory period prevents the spike from propagating backwards and, at the same time, stops the generation of further spikes, in order to fire one spike at a time.

This phenomenon shows strong similarities with the concept of *polaron* by H. Fröhlich [22, 23, 24, 25, 26, 27] which describes an electron that moves with its field of deformation (see also RP Feynman, 1954, [28, 29]). In that case, the carrier together with the induced deformation can be considered as one entity: a *quasi-particle* called *polaron*. In the present case, following H. Fröhlich’s concept of *polaron*, we define the spike wave function Ψ_{spike} by exploiting the formalism of the “*Produkt-Ansatz*” by L. D. Landau (1933) [30] as the following (in kets):

$$|\Psi_{spike}\rangle = |\varphi(\mathbf{r})_{carrier}\rangle |field\rangle := |\varphi(\mathbf{r})_{carrier}\rangle |Ising\rangle \quad (8)$$

Where $|\varphi(\mathbf{r})_{carrier}\rangle$ is the carrier wave function while $|field\rangle$ is the field of the Ising Machine and \mathbf{r} is the position operator of the carrier along the axon axis in the direction of propagation of the carrier.

The total Fröhlich Hamiltonian function of our model will be given by:

$$H = H_{Carrier} + H_{Ising} + H_{Carrier*Ising} = \frac{\mathbf{p}^2}{2m_c} + H_{Ising} + H_{Carrier*Ising} \quad (9)$$

Where \mathbf{p} is the canonically conjugate momentum operator of the carrier of mass m_c and H_{Ising} the Hamiltonian function (1). In this way, we can interpret the spike as a quasi-particle which represents the carrier together with the induced deformation on the nerve cell membrane.

We call this quasi-particle *nuon* and denote it with the letter \tilde{n} . The statistical field theory that foresees the concept of nuon will for brevity be called SFT [\tilde{n}].

As a first approximation, if we consider the density of ion channels on the axonal membrane of non-myelinated axons almost constant [6, 31, 32, 33, 34], we can neglect

the composition terms $H_{Carrier*Ising}$ in (9) after the trigger of the first spike, because the process is ruled only by Ising's machines.

Therefore, we consider the process of generation and transmission of a spike for a time $t > \tau$, where τ is the generation time of each spike by each pair (Na/K) of Ising Machines. If we indicate with s the coordinate along with the axis of the axon (which coincides with the axis of the coaxial annular sections), then each section (housing a pair of Ising Machines Na/K) will be traveled in a time t by the coordinate $s = s(t)$. Therefore, the velocity $v = ds/dt$ of the neuron will be given by the limit of the difference quotient $\Delta s/\Delta t$ with $\Delta t \neq 0$. Our choice of the one-dimensional Ising model is thus clear. Finally, we will have

$$H \approx \frac{p^2}{2m_c} + H_{Ising} \quad (10)$$

Discussion

The saltatory conduction

An application case of neurological interest is that of the so-called ‘‘saltatory conduction’’ in myelinated axons. Measures of the average velocity of spikes in non-myelinated axons are between 0, 5 and 10 m/s, while in myelinated axons they can even exceed circa 150 m/s [6, 31, 32, 33, 34, 35]. Multiple Sclerosis (MS) is a serious pathology of the central nervous system (CNS) characterized by a complex of clinical disorders caused by the bad conduction of spikes, as a consequence of damage and/or total or partial loss of the myelin sheath (demyelination) due to the inflammation of the axon pathways. [6, 31, 32, 33, 34, 35, 36]. The study of saltatory conduction is therefore crucial to understand and deal with these serious diseases. Saltatory conduction is described by means of the ‘‘cable theory’’. Let's now see how some relations derived from cable theory can be interpreted in the context of SFT[\tilde{n}]. We can model the myelin sheath as composed of a series of concentric thin cylindrical surfaces of length L , capacity per unit of area c_m and thickness d_m distributed from the radius a_1 of the axon core to the external radius a_2 , that is to the axon radius (See next Fig. 10).

We will then have a total capacity C_m (series) given by the following relations [8]

$$\frac{1}{C_m} = \frac{1}{c_m 2\pi d_m L} \int_{a_1}^{a_2} \frac{da}{a} = \frac{\ln\left(\frac{a_2}{a_1}\right)}{c_m 2\pi d_m L} \quad (11)$$

Where the myelin sheath extends from the radius a_1 of the axon core to the outer radius a_2 , that is to the axon radius (See Fig. 10d/e).

Performing the (linear) cable theory, we obtain the diffusion equation:

$$\frac{C_m}{L} \frac{\partial v}{\partial t} = \frac{\pi a_1^2}{r_L} \frac{\partial^2 v}{\partial x^2} \quad (12)$$

The diffusion coefficient is:

$$D = \frac{\pi a_1^2 L}{c_m r_L} = \frac{a_1^2 \ln\left(\frac{a_2}{a_1}\right)}{2 c_m r_L d_m} \quad (13)$$

Where r_L is the intracellular resistivity. The optimal value of the internal radius a_1 - which maximizes the diffusion constant- is $a_1 \sim 0.6 a_2$ [8]. In the case of a myelinated axon the propagation velocity is thus proportional to the outer radius a_2 , that is to the axon radius, while for an unmyelinated axon it is proportional to the square root of the axon radius (a_2) [8]

$$v \sim a_2 \quad (14)$$

Let us show with an example the versatility of the particle description of nerve impulses. Here we exploit the physics of particle accelerators [37, 38] because from our point of view the functionality of a myelinated axon is that of a (micro) linear particle accelerator (μ LINAC).

The myelinated regions behave like Faraday cages (drift tubes) while at the gaps of the nodes of Ranvier there is a non-zero electric field that provides the acceleration of the particle along the axon (see figure 10f). During the acceleration the velocity increases monotonically. In the i th drift tube the velocity v_i is reached. Now, considering the effective mass $m_{\bar{n}}$ of a nuon, we thus have an energy:

$$E_i = \frac{1}{2} m_{\bar{n}} v_i^2 \quad (15)$$

From cable theory we deduce that the average velocity is proportional to the radius of the myelin axon (14). In this way, we can estimate the effective mass and charge of the nuon and the modulus of the electric field at the nodes of Ranvier. This is a crucial result. To explain the biophysical mechanism of demyelinating pathologies we can use the nuon model because it provides advantages over the “classic” electrophysiological description. However, the model is *congruent* with the “classic” description because a spike is the electrophysiological trace and probe of the passage of a nuon.

Demyelination, due to the interruption of the paranodal myelin circuits, causes the dispersion of all the ion channels, pumps and exchangers along the axon [6, 31, 32, 33, 34, 35, 36, 39]. Sodium overload causes axonal calcium to reach toxic levels and so on [31]. As the conduction velocity in normal conditions (up to circa 150 m/s) is much higher than the velocity in pathological conditions (about 5 or 10 m/s), we can predict that, in pathological conditions, the resultant of the forces on the system will contain a finite set of deterministic dissipative fields acting on the demyelinated axon, generating instabilities and losses (that we can think as in the damaged drift tubes of our μ LINAC). This model can also offer an operative tool characterized by self-similarity and reproducibility properties for polytype diffusion, since the etiology of the disease is presumably caused by a pathological (inflammatory) process that affects the entire organ system. Knowledge and measurement of these dissipative fields can therefore lead to significant progress in the study and treatment of neurodegenerative and demyelinating diseases. Furthermore, our considerations on the dissipative field model can be used to

define a special circuitry intended to integrate the equivalent models (See Richardson [40]).

Conclusions and possible insights

In this work we found a particle description of action potentials, based on considerations of statistical mechanics of complex and disordered systems, independently of electrophysiological models, such as Hodgkin-Huxley (HH).

Nevertheless, as soon as we consider the action potential as the electro-physiological trace of the nuon, we thus have the opportunity to exploit those different points of view to describe the generation and propagation of nerve impulses, especially when classic electrophysiological models break down. We can strictly speak of a dual representation of which we have established the theoretical bases. In this case, SFT [\tilde{n}] is a powerful tool that allows us to use the techniques and results of theoretical and general physics [41,42]. As we have just pointed out in the previous paragraph for the case of saltatory conduction, it is advantageous to use both representations. But we expect the dual representation to be useful in many other cases as well. Functional Magnetic Resonance (fMRI) can be integrated by specific hardware devices and algorithms currently employed in heavy particle physics in order to obtain real-time velocity field maps, even led by connectomes [43]. A detailed integrated real time imaging is therefore suitable to study a non-active area of the brain (i.e. in the presence of ischemia, injury, ictus, neurodegenerative pathology or tumor), by considering an "activity" tensor dependent on the nuon frequencies and fluxes defined on a dendritic density field [44]. Furthermore, the study of the activity with the particle model can try to explain evolutionary puzzles related to multiple sclerosis, difficult to solve with electrophysiological models (see [45]). Other possible applications will exploit "nuon coding" [7] to study and develop complex networks, quantum computing, artificial intelligence, machine and deep learning, cryptography, ultra-fast lines for entanglement experiments and so on. A particle model of synaptic transmission through a "nuon number" conservation law may be also derived analogically from particle physics experiments and theory.

List of abbreviations

HH : Hodgkin-Huxley models; INM: Ising Neural Machine;

SFT [\tilde{n}]: Statistical Field Theory of the Transmission of Nerve Impulses;

fMRI : functional Nuclear Magnetic Resonance.

Declarations

Author's contributions

GZdB developed the theory and wrote the manuscript.

Ethics approval and consent to participate

Not applicable.

Consent for publication

Not applicable

Availability of data and material

Not applicable

Funding

Not applicable. The author received no specific funding for this work, as it is a voluntary work for the fight against the COVID-19 Pandemic.

Competing interests

Not applicable

Acknowledgements

Not applicable

References

1. Hodgkin, A.L., Huxley, A.F.: Currents carried by sodium and potassium ions through the membrane of the giant axon of Loligo. *J. Physiol* **116**, 449–472 (1952)
2. Hodgkin, A.L., Huxley, A.F.: The components of membrane conductance in the giant axon of Loligo. *J. Physiol* **116**, 473–496 (1952)
3. Hodgkin, A.L., Huxley, A.F.: The dual effect of membrane potential on sodium conductance in the giant axon of Loligo. *J. Physiol* **116**, 497–506 (1952)
4. Hodgkin, A.L., Huxley, A.F.: A quantitative description of membrane current and its application to conduction and excitation in nerve. *J. Physiol* **116**, 507–544 (1952)
5. Hille, B.: *Ion Channels of Excitable Membranes*. Sinauer Associates Inc, Sunderland, MA, USA (2001)
6. Purves, D., et al., *Neuroscience*, Sinauer Associates Inc, Sunderland, MA, USA (2004)
7. Gerstner, W., et al.: *Neuronal Dynamics*. Cambridge University Press, Cambridge UK (2014)
8. Dayan, P., Abbott, L.F., et al.: *Theoretical Neuroscience. Computational and Mathematical Modeling of Neural Systems*. The MIT Press, Cambridge, Massachusetts (2001)
9. Neher, E., Sakmann, B.: Single-channel currents recorded from membrane of denervated frog muscle fibres. *Nature (Lond.)* **260**, 779–802 (1976)
10. Mezard, M., Parisi, G., Virasoro, M.: *Spin Glass Theory and Beyond*. World Scientific, (1987)
11. Fischer, K.H., Hertz, J.A.: *Spin Glasses*. In: et al.(ed.) Cambridge University Press, (1991)
12. Edwards, S.F., Anderson, P.W.: Theory of spin glasses. *J. Phys. F: Metal. Phys* **5** (1975)
13. Huang, K.: *Statistical Mechanics*. In: Sons, J.W.. (ed.) (1987)
14. Hopfield, J.J.: Neural networks and physical systems with emergent collective computational abilities. *Proc. Natl. Acad. Sci. USA* **79**, 2554–2558 (1982)

15. Amit, D.J., Gutfreund, H.: Spin-glass models of neural networks. *Physical Review A* **32**(2), 1007–1018 (1985)
16. Zangari, G.: Category Calculus System and applications - Patent U.S. Copyright Office n. TXU001773372
17. Zangari, G.; Modelli Matematici per i Rivelatori di Particelle della Fisica Nucleare. Book. ISBN: 9798663330961 (2020)
18. Zangari, G.; Analisi Statistica di Massima Congruenza applicata all'emissione di radiazione di sincrotrone: il caso della ϕ -Factory Da ϕ ne. Book. ISBN: 9798673324172 (2020)
19. Zangari, G.: The unsuspected “bodyguards” of Red Blood Cells. Zenodo. <http://doi.org/10.5281/zenodo.3999291> (2020).
20. Klitzing, R.: “Quasi-Periodic Structures”, “Polytopes” in “Snubs. Alternated Facetings & Stott-Coxeter-Dynkin Diagrams” in *Symmetry: Culture and Science* **21**, 329–344 (2010)
21. Klitzing, R.: Polytopes and their Incident Matrices (2019). <https://bendwavy.org/klitzing/home.htm>
22. Devreese, J.T.: Polarons. In: et al.(ed.) *Encyclopaedia of Applied Physics*, vol. 14, pp. 383–409. Wiley Publishers, Inc, (1996)
23. Pekar, S.I.: “Research in electron theory of crystals”, Moscow: Gostekhizdat-German translation. In: *Research in Electron Theory of Crystals*. Akademie Verlag, (1951)
24. Fröhlich, H.: Theory of electric breakdown in ionic crystals. *Proc. Roy. Soc. London, A* **160**, 230–230 (1937)
25. Fröhlich, H. *Advances in Physics* **3**, 325–325 (1954)
26. Fröhlich, H., 6th Ampère Colloquium Supplement: 6th Ampère Colloquium Supplement. *Archives des Sciences de Genève* **10**, 5–6 (1957)
27. Fröhlich, H., Sewell, G.L.: -. *Proc. Phys. Soc* **74**, 643–647 (1959)
28. Feynman, R.P.: Slow Electrons in a Polar Crystal. *Physical Review* **97**(3), 660–665 (1955)
29. Feynman, R.P.: Mobility of Slow Electrons in a polar Crystal. *Physical Review* **127**(4), 1004–1017 (1962)
30. Landau, L.D.: *Collected Papers of L. D. Landau 1St Edition* . In: Haar, D.T. (ed.) Pergamon, (1965)
31. Inouye, H., Kirschner, D.A.: Membrane interactions in nerve myelin: I. Determination of surface charge from effects of pH and ionic strength on period”. *Biophys. J* **53**(2), 235–245 (1988)
32. Inouye, H., Kirschner, D.A.: Membrane interactions in nerve myelin: II. Determination of surface charge from biochemical data”. *Biophys. J* **53**(2), 247–260 (1988)
33. Karthigasan, J., Kirschner, D.A.: “membrane interactions are altered in myelin isolated from central and peripheral nervous system tissues. *J. Neurochem* **51**(1), 228–236 (1988)
34. Fields, D.: A new mechanism of nervous system plasticity: activity-dependent myelination”. *Nature Reviews Neuroscience* **16**, 756–767 (2015)
35. Karthigasan, J., Kirschner, D.A.: “membrane interactions are altered in myelin isolated from central and peripheral nervous system tissues. *J. Neurochem* **51**(1), 228–236 (1988)
36. Alizadeh, A., Scott, M., Dyck, S., Karimi-Abdolrezaee, q.: Myelin damage and

- repair in pathologic CNS: challenges and prospects. *Frontiers in Molecular Neuroscience* **8**, 35–35 (2015)
37. Wille, K.: *The Physics of Particle Accelerators*. In: Press, O.U., et al.(eds.) *The Physics of Particle Accelerators*. Oxford University Press, (2000)
 38. Alesini, D.: *Introduction to Accelerator Physics - Linear Accelerators*. CERN Accelerator School (2016)
 39. Desmazieres, A., Zonta, B., Zhang, A., Lai-Man, N., Wu, D.L., Sherman, P.J., Brophy, q.: Differential Stability of PNS and CNS Nodal Complexes When Neuronal Neurofascin Is Lost. *Journal of Neuroscience* **34**(15), 5083–5088 (2014)
 40. Richardson, A.G., McIntyre, C.C., Grill, W.M.: Modelling the effects of electric fields on nerve fibres: Influence of the myelin sheath. *Medical & Biological Engineering & Computing* **38**(4), 438–446 (2000)
 41. Dybalsky, W., Spohn, H.: Effective mass of the polaron -revisited. *ArXiv.org* (Cornell University) (2019)
 42. Zavjalov, S., Autti, V.B., & P, J.E., Heikkinen: Measurements of the anisotropic mass of magnons confined in a harmonic trap in superfluid $^3\text{He-B}$ ". *JETP Letters* **101**, 802–807 (2015)
 43. Oh, J.A.S.W., Harris, L., Ng, B., Winslow, N., Cain, S., Mihalas, Q., Wang, C., Lau, L., Kuan, A.M., Henry, M.T., Mortrud, B., Ouellette, q., Nguyen, S.A.T.N., Sorensen, C.R., Slaughterbeck, W., Wakeman, Y., Li, D., Feng, A., Ho, E., Nicholas, K.E., Hirokawa, P., Bohn, K.M., Joines, H., Peng, M.J., Hawrylycz, J.W., Phillips, J.G., Hohmann, P., Wahnoutka, C.R., Gerfen, C., Koch, A., Bernard, C., Dang, A.R., & Hongkui, q.J., Zeng, q.: A mesoscale connectome of the mouse brain". *Nature* **508**, 207–214 (2014)
 44. Cuntz, H.: The Dendritic Density Field of a Cortical Pyramidal Cell. *Frontiers in Neuroanatomy* **6** (2012)
 45. Bove, R.M.: Why monkeys do not get multiple sclerosis (spontaneously)? *Evolution, Medicine and Public Health* [2018] pp. 43.59, 43–59 (2018)
 46. University of Yale, USA Myelinated Axon EM. <http://medcell.med.yale.edu/histology/nervous\ system\ lab/myelinated\ axon\ em.php>
 47. Peter Brophy, Wellcome Collection: Node of Ranvier. <https://wellcomecollection.org/works/p9pzeqec>

Figures

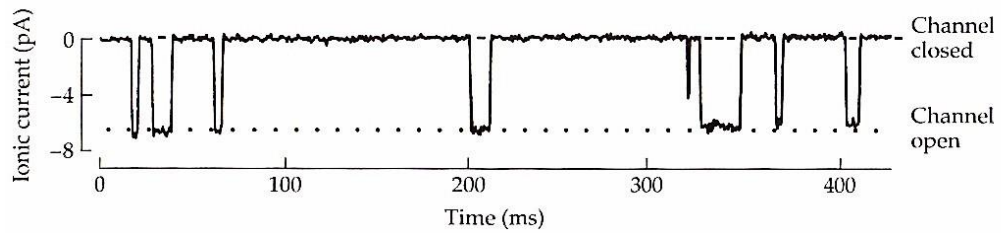


Figure 1 The flow of an ionic current of the order of 6.6 pA through a small axonal membrane element shows eight ion channel openings (corresponding to a flow of 4.1×10^7 ions per second through a single pore). (Courtesy of B. Hille, [5]).

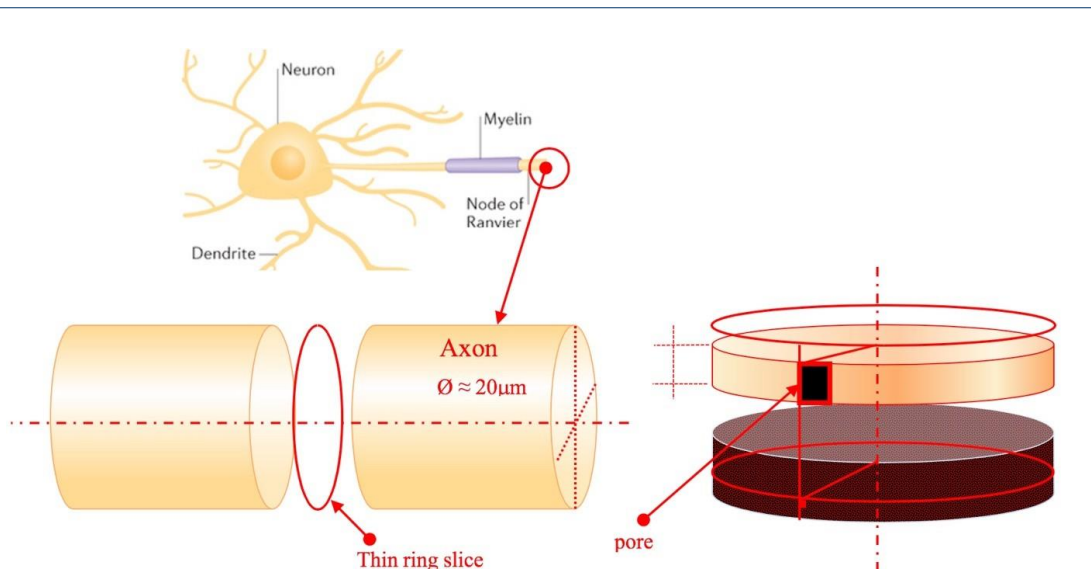


Figure 2 N voltage-dependent ion channels on an elementary region (slice) of an axon made by a thin ring of radius $\rho \sim 10\mu\text{m}$ and thickness $h \sim 1\text{nm}$.

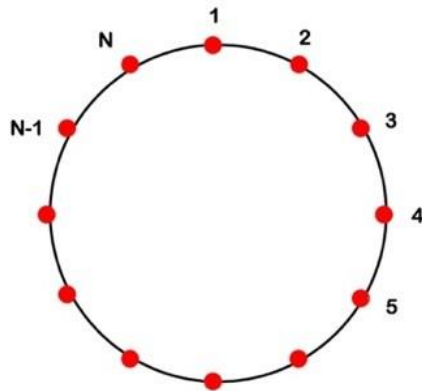


Figure 3 Topology of the one-dimensional Ising model, after K. Huang [13]

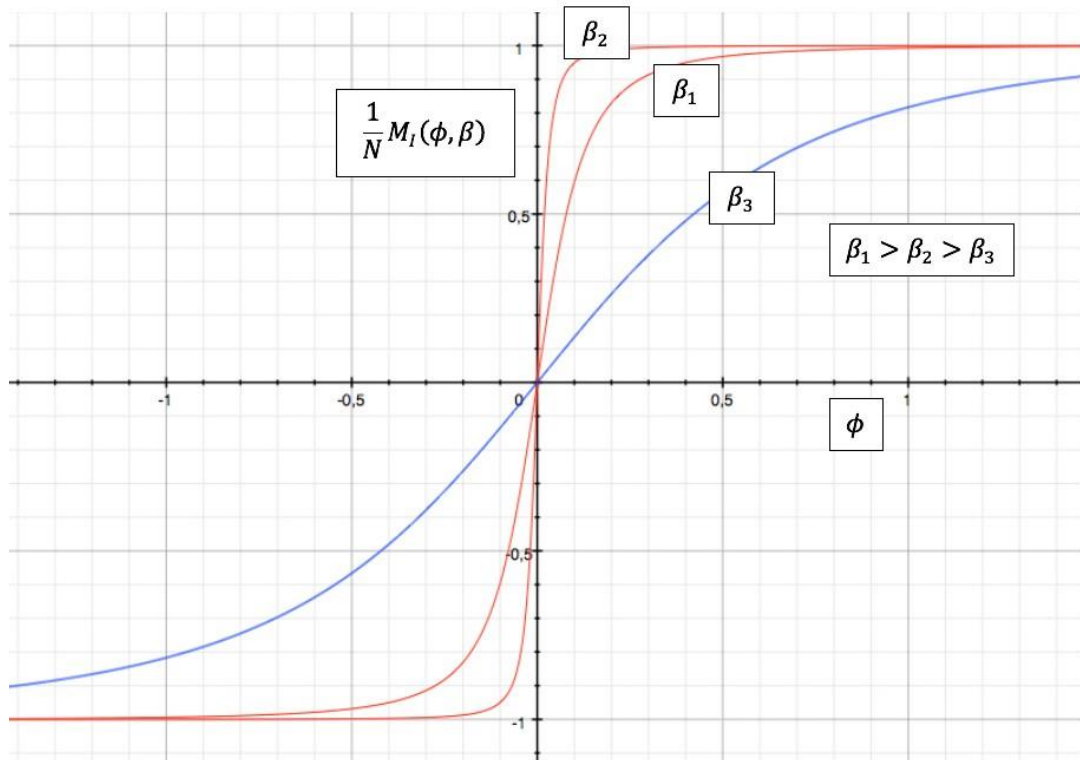


Figure 4 Spin magnetization in the one-dimensional Ising Model for three different “temperatures” and $J = 1$.

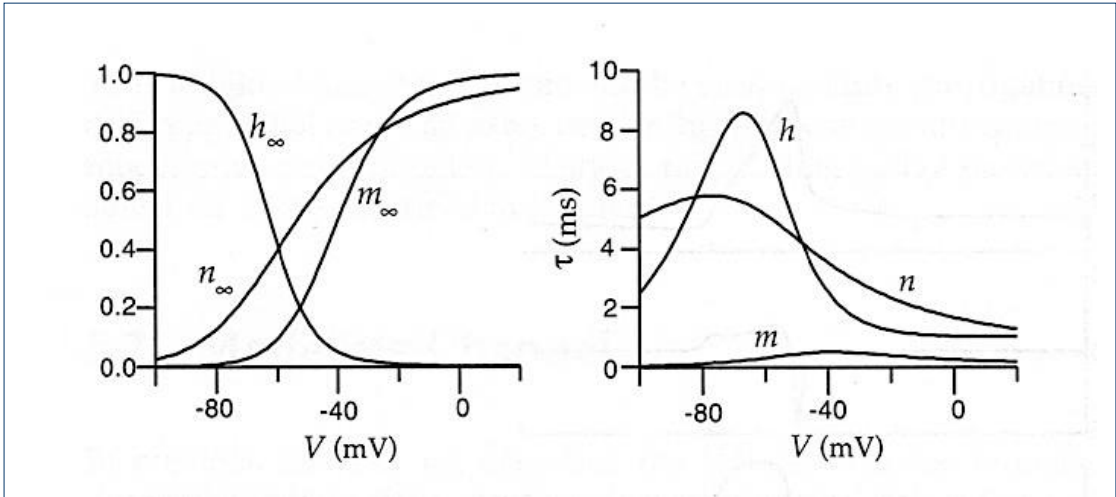


Figure 5 Characteristic limit ratios as a function of membrane potential in the HH model. The figure on the left shows the limit functions for activating the K^+ conductance (n_∞) and the activation and inactivation functions for the Na^+ conductance (m_∞ , h_∞). The relative time constants (as a function of potential) are shown on the right. (courtesy of P. Dayan et Al., [8])

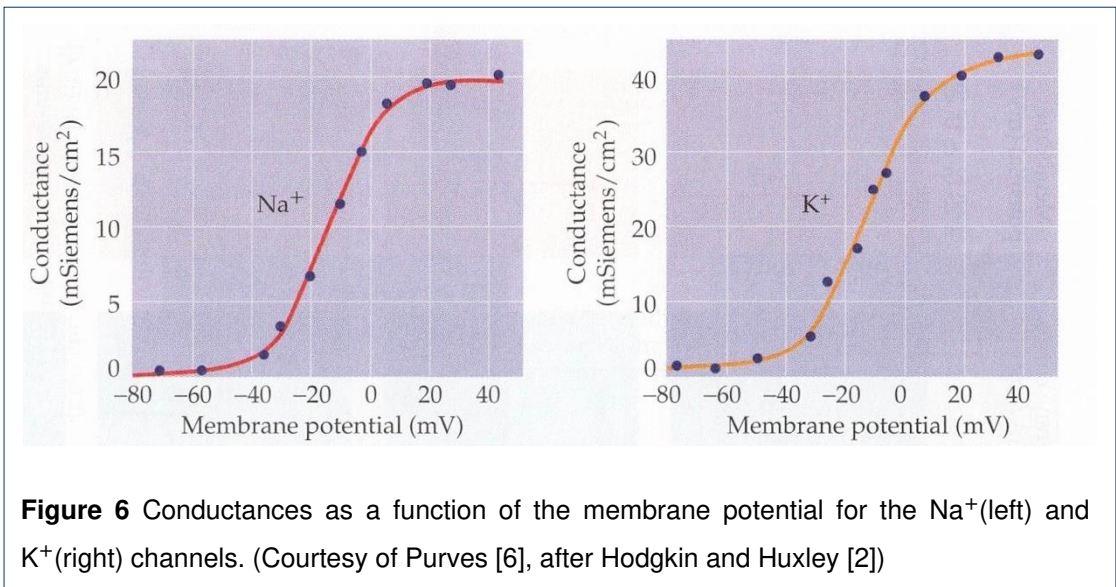


Figure 6 Conductances as a function of the membrane potential for the Na^+ (left) and K^+ (right) channels. (Courtesy of Purves [6], after Hodgkin and Huxley [2])

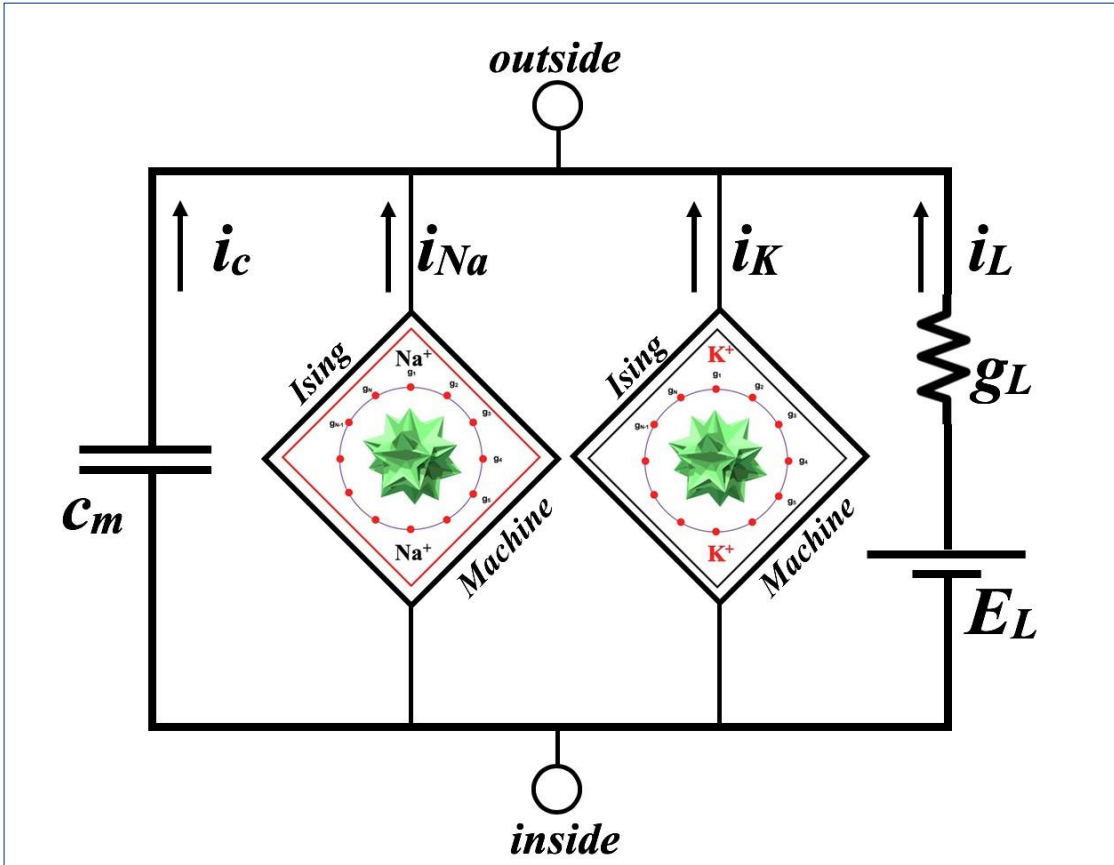
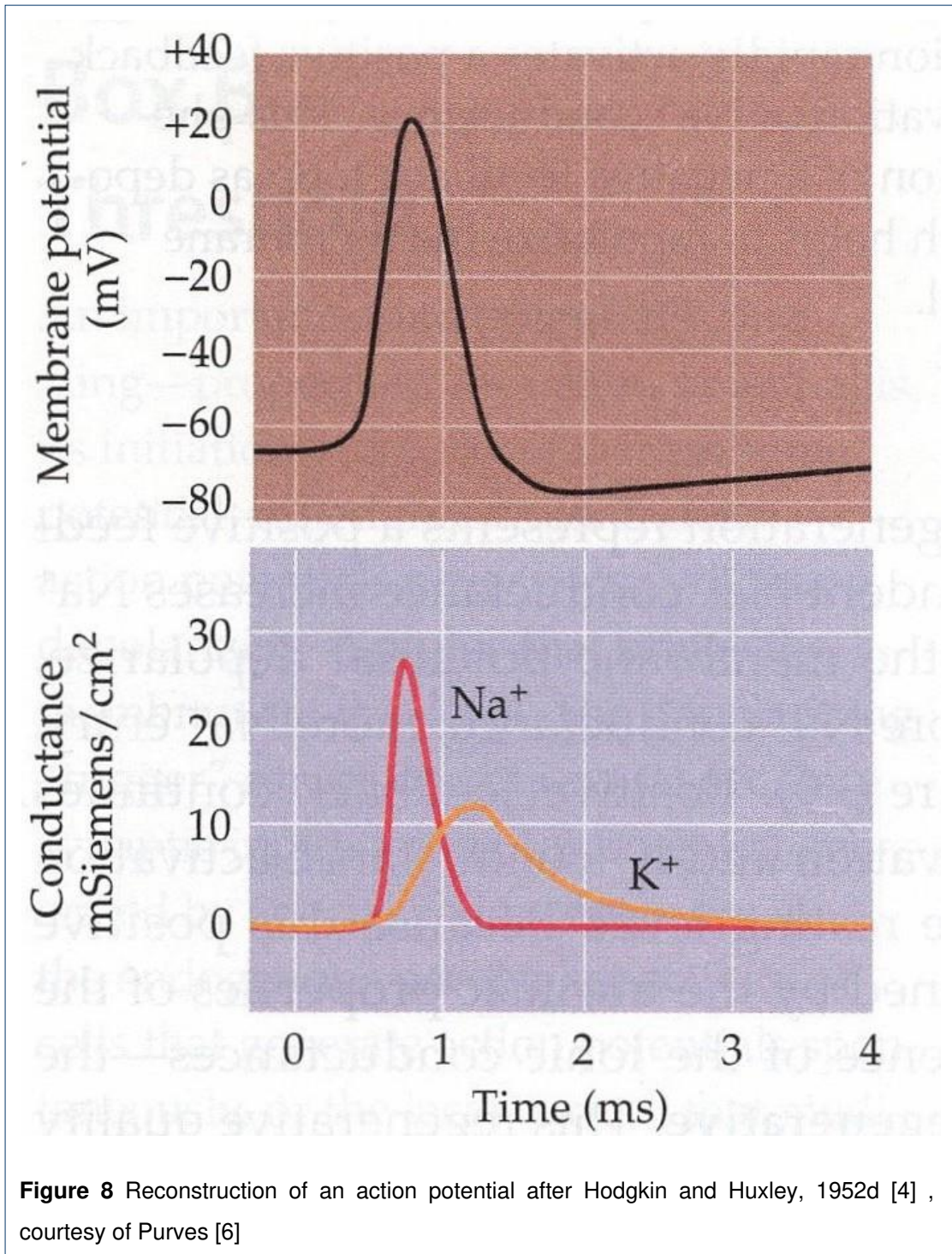


Figure 7 The “Ising Neural Machine”. The equivalent single compartment circuit containing two stochastic elements called “Ising Neural Machines”, respectively for the Na^+ channels and for the K^+ channels^[1]. By “inside” and “outside” is meant inside and outside the nerve cell membrane. The specific capacity of the membrane is indicated as c_m while i_L , g_L and E_L indicate respectively the “leakage current”^[2] per unit area, the leakage conductance and potential. The currents leaving the two Ising machines are total currents (per unit area).



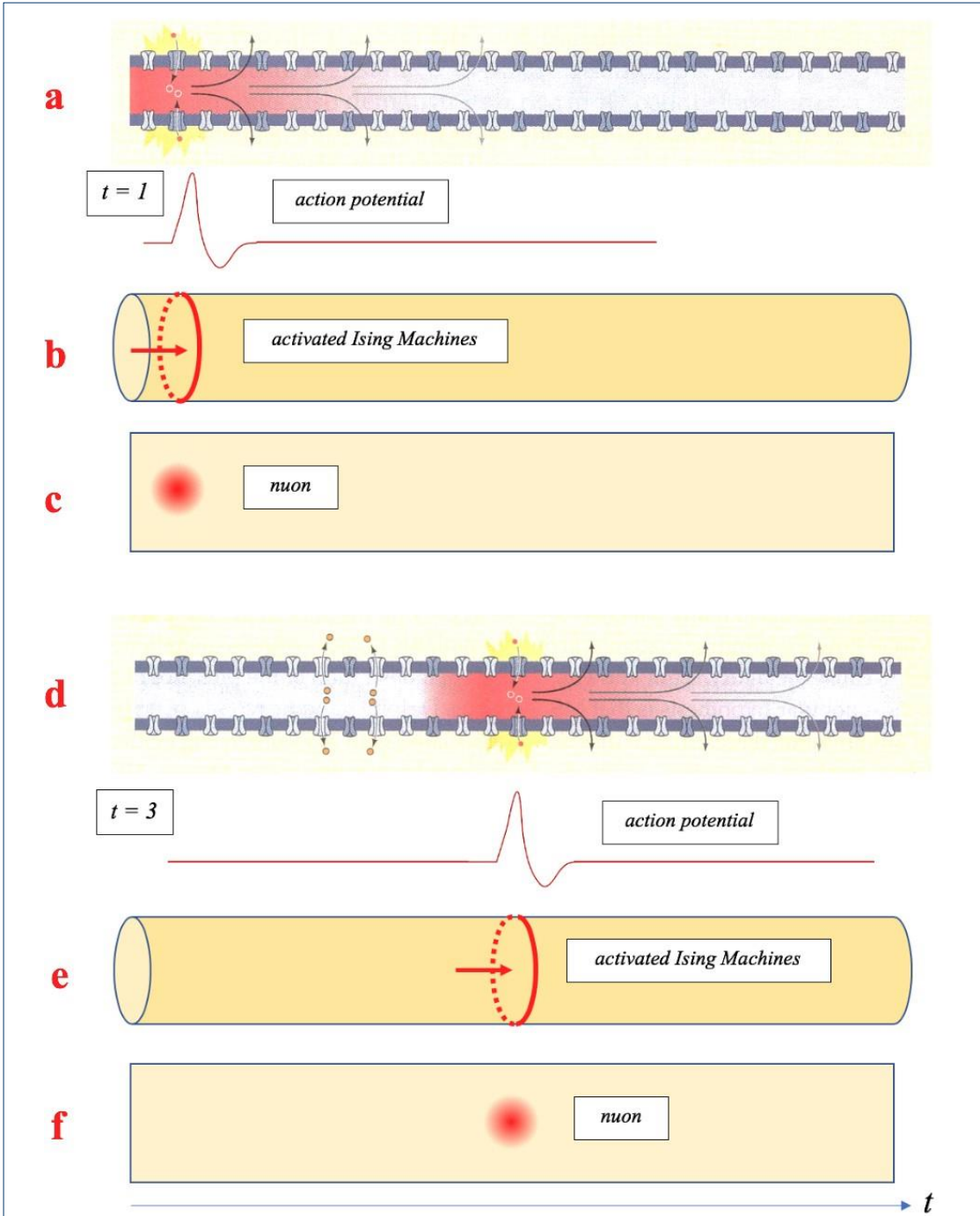


Figure 9 Spikes and nuons. Figures (9a) and (9d) (modified after D. Purves, [6]), show the motion of a spike for $t = 1$ and $t = 3$.

Figures (9b) and (9e) show the trigger of a pair of Na^+/K^+ Ising machines housed in annular regions of the membrane for $t = 1$ and $t = 3$.

Figures (9c) and (9f) show the motion of a nuon along the axon for $t = 1$ and $t = 3$.

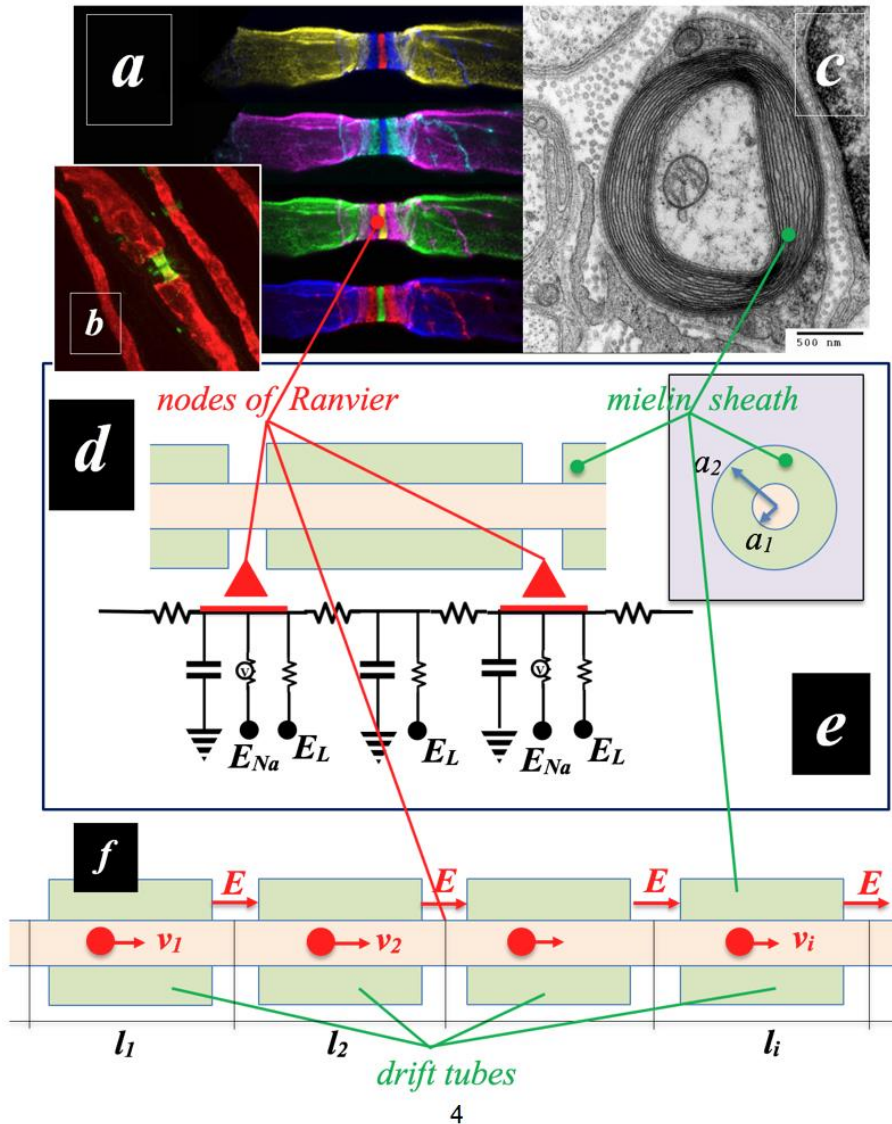


Figure 10 Nodes of Ranvier and Myelin Sheath.

Fig. 10a- Courtesy of Anne Desmazieres et Al. [39] .

Fig. 10b - Courtesy of Prof. Peter Brophy [47] .

Fig. 10c- The structure of the myelin sheath is clearly visible in the electron microscope image. Courtesy by the University of Cambridge, UK. [46].

Fig. 10d/e - The nodes of Ranvier and the myelinated regions of an axon are represented as an equivalent circuit within an inter-compartmental model, modified after F. Dayan et al. [8] .

Figure 10f - Schematic of our model of a μ LINAC, where an electric field acts in the nodes of Ranvier and accelerates the nuons in the myelinated sections that behave like drift tubes.

Figures

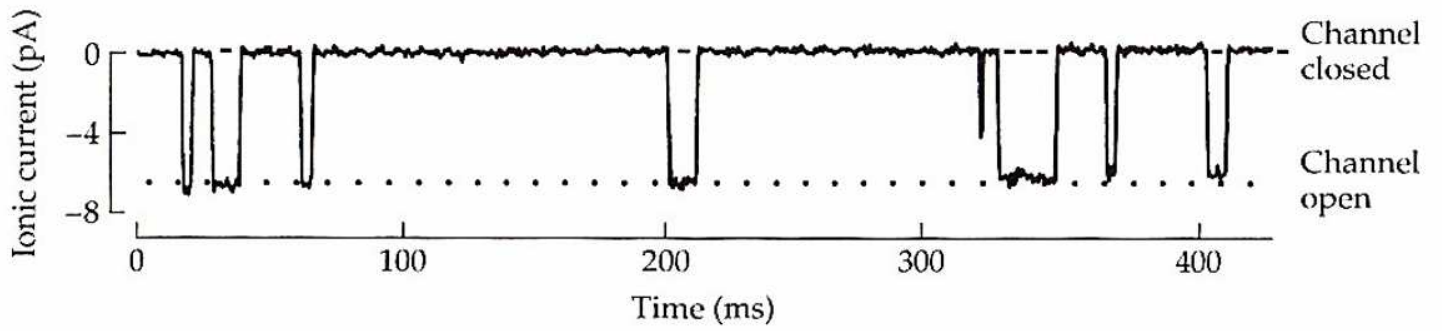


Figure 1

The flow of an ionic current of the order of 6.6 pA through a small axonal membrane element shows eight ion channel openings (corresponding to a flow of 4.1×10^7 ions per second through a single pore). (Courtesy of B. Hille, [5]).

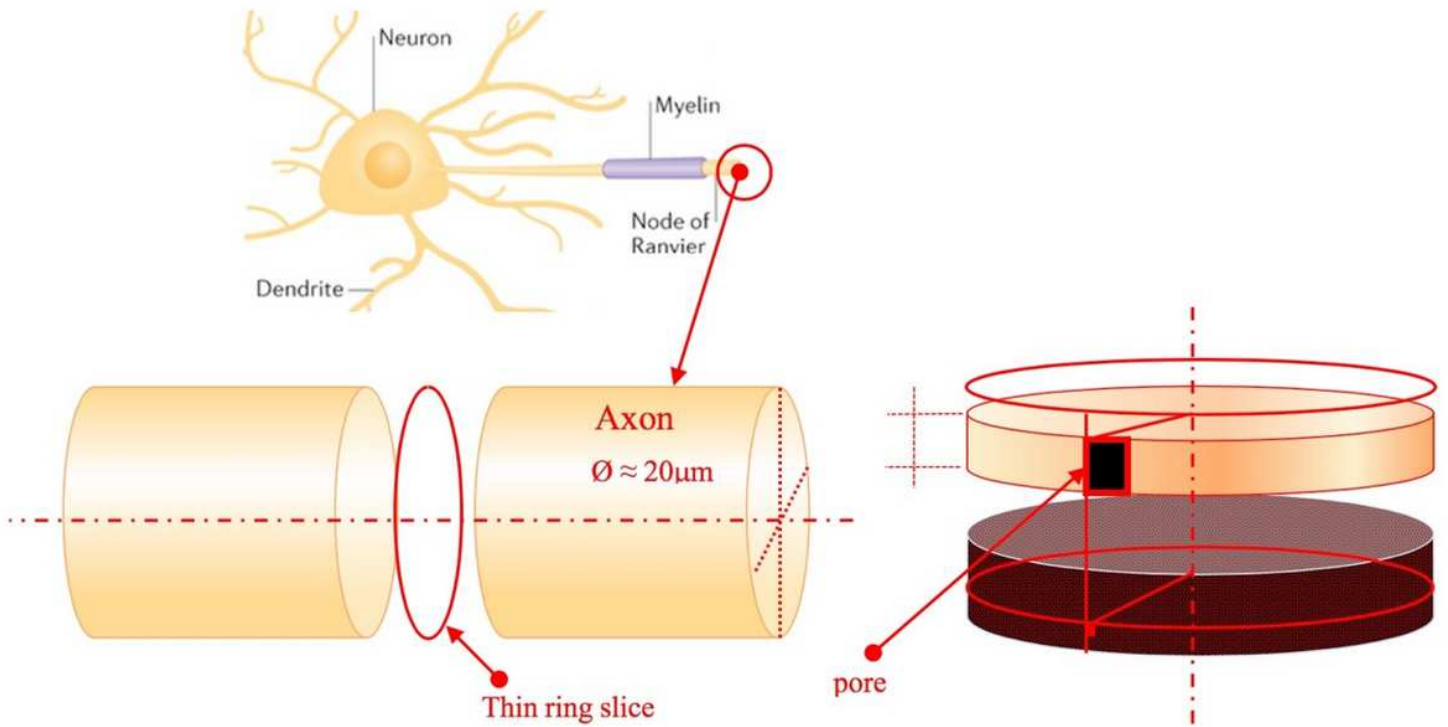


Figure 2

N voltage-dependent ion channels on an elementary region (slice) of an axon made by a thin ring of radius $\rho \approx 10\mu\text{m}$ and thickness $h \approx 1\text{nm}$.

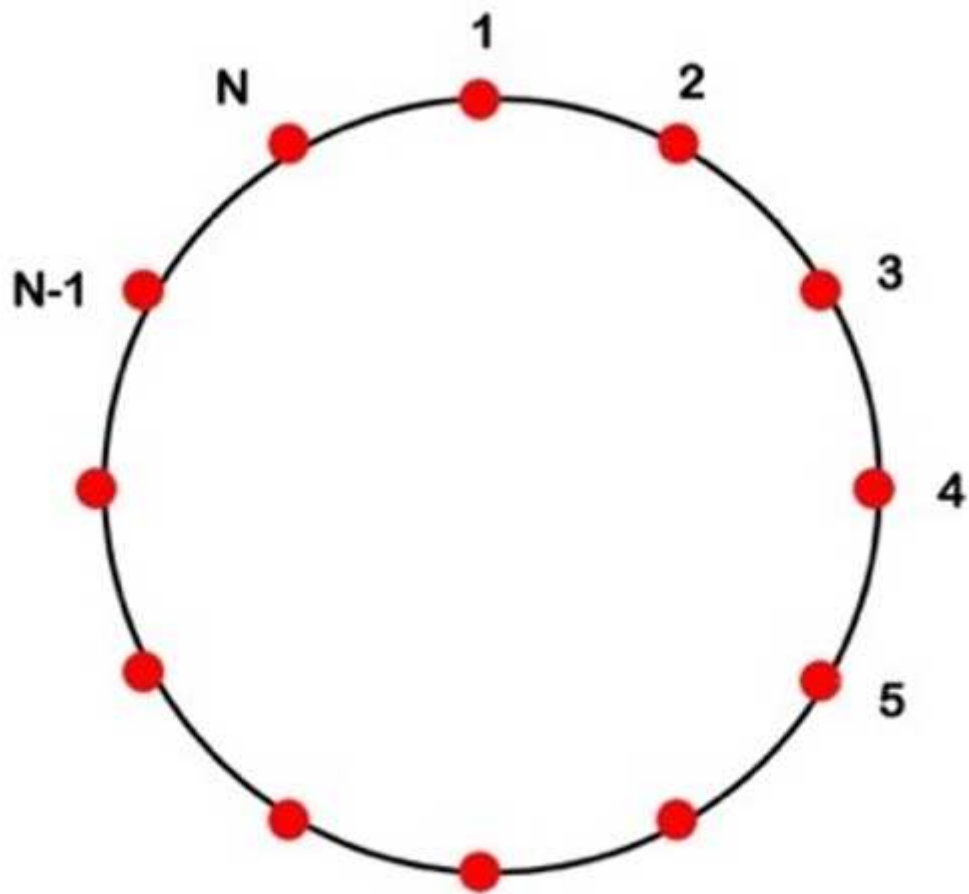


Figure 3

Topology of the one-dimensional Ising model, after K. Huang [13]

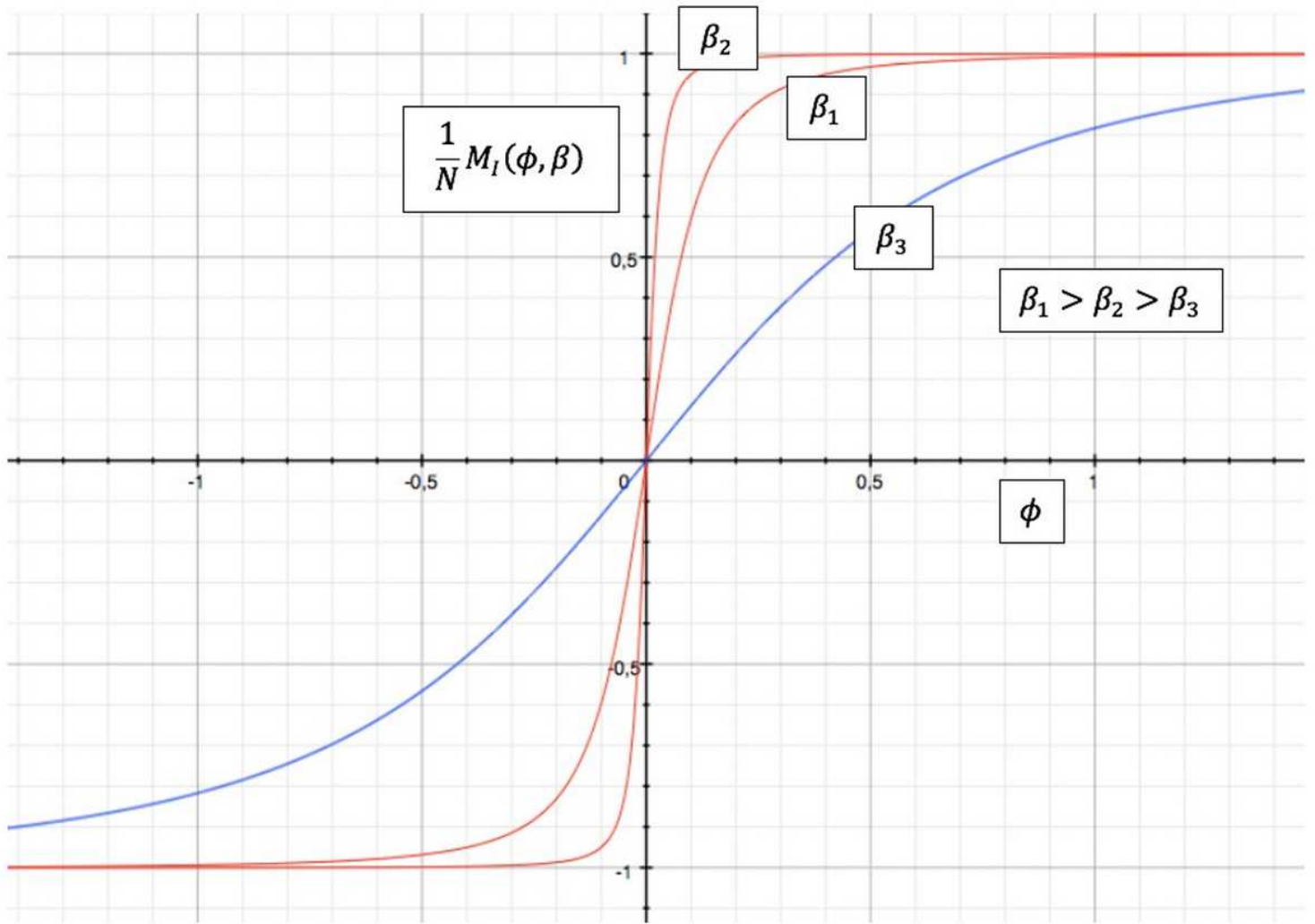


Figure 4

Spin magnetization in the one-dimensional Ising Model for three different “temperatures” and $J = 1$.

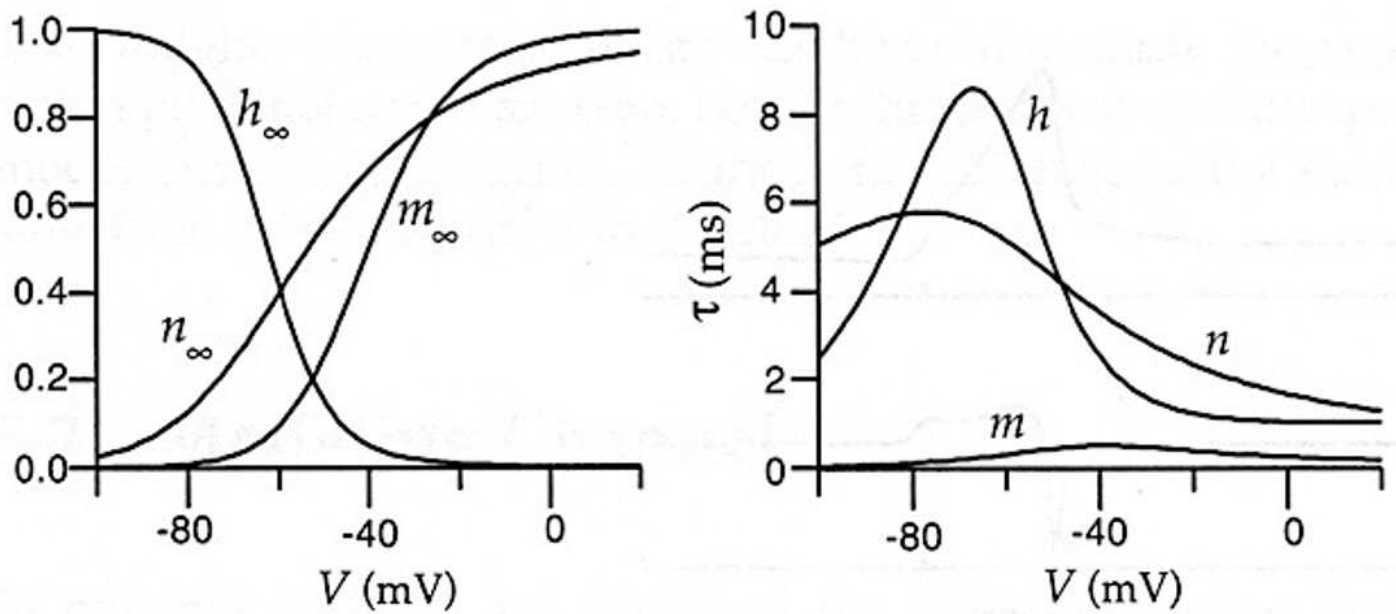


Figure 5

Characteristic limit ratios as a function of membrane potential in the HH model. The figure on the left shows the limit functions for activating the K⁺ conductance (n_{∞}) and the activation and inactivation functions for the Na⁺ conductance (m_{∞} , h_{∞}). The relative time constants (as a function of potential) are shown on the right. (courtesy of P. Dayan et Al., [8])

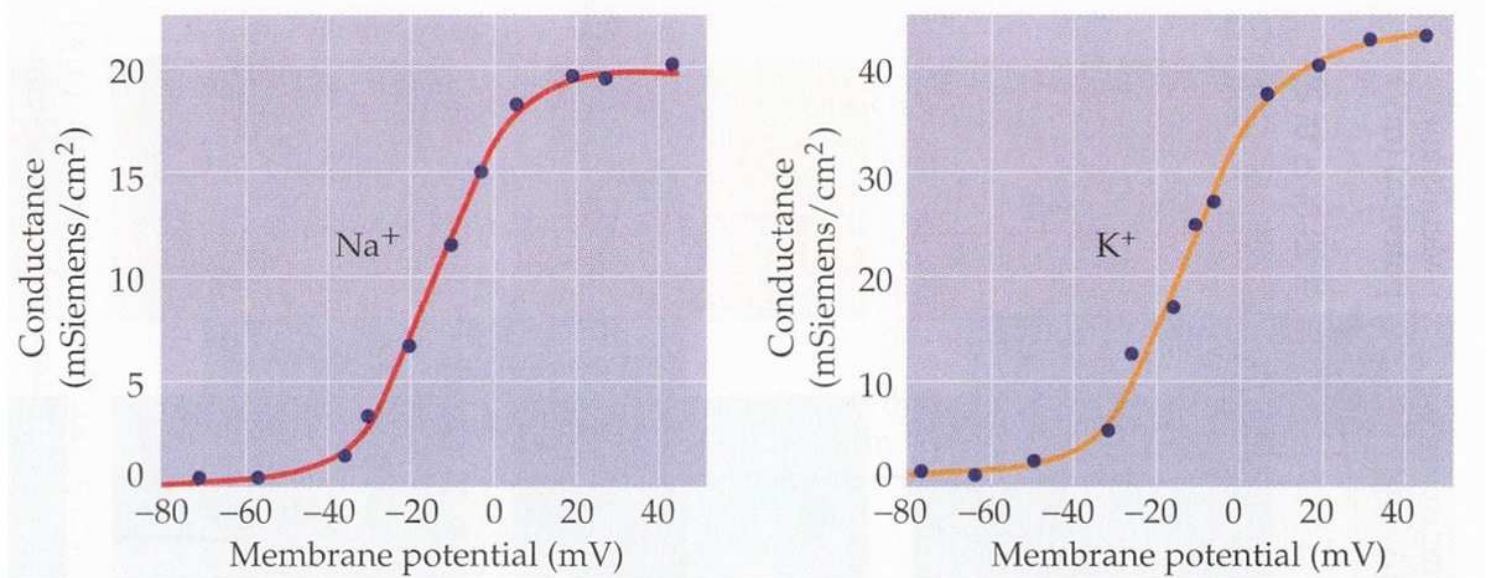


Figure 6

Conductances as a function of the membrane potential for the Na⁺(left) and K⁺(right) channels. (Courtesy of Purves [6], after Hodgkin and Huxley [2])

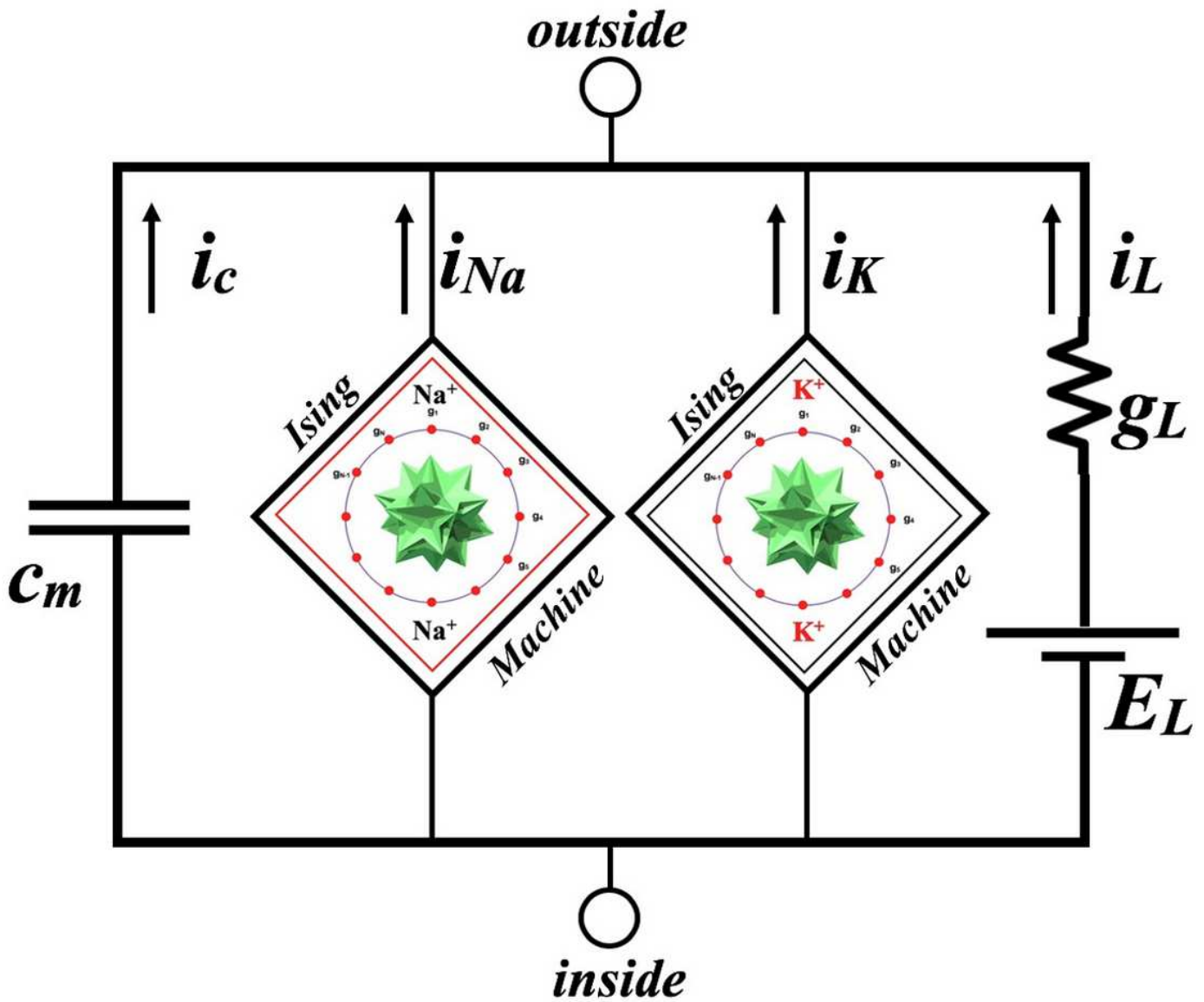


Figure 7

The “Ising Neural Machine”. The equivalent single compartment circuit containing two stochastic elements called “Ising Neural Machines”, respectively for the Na^+ -channels and for the K^+ -channels[1]. By “inside” and “outside” is meant inside and outside the nerve cell membrane. The specific capacity of the membrane is indicated as c_m while i_L , g_L and E_L indicate respectively the “leakage current”[2] per unit area, the leakage conductance and potential. The currents leaving the two Ising machines are total currents (per unit area).

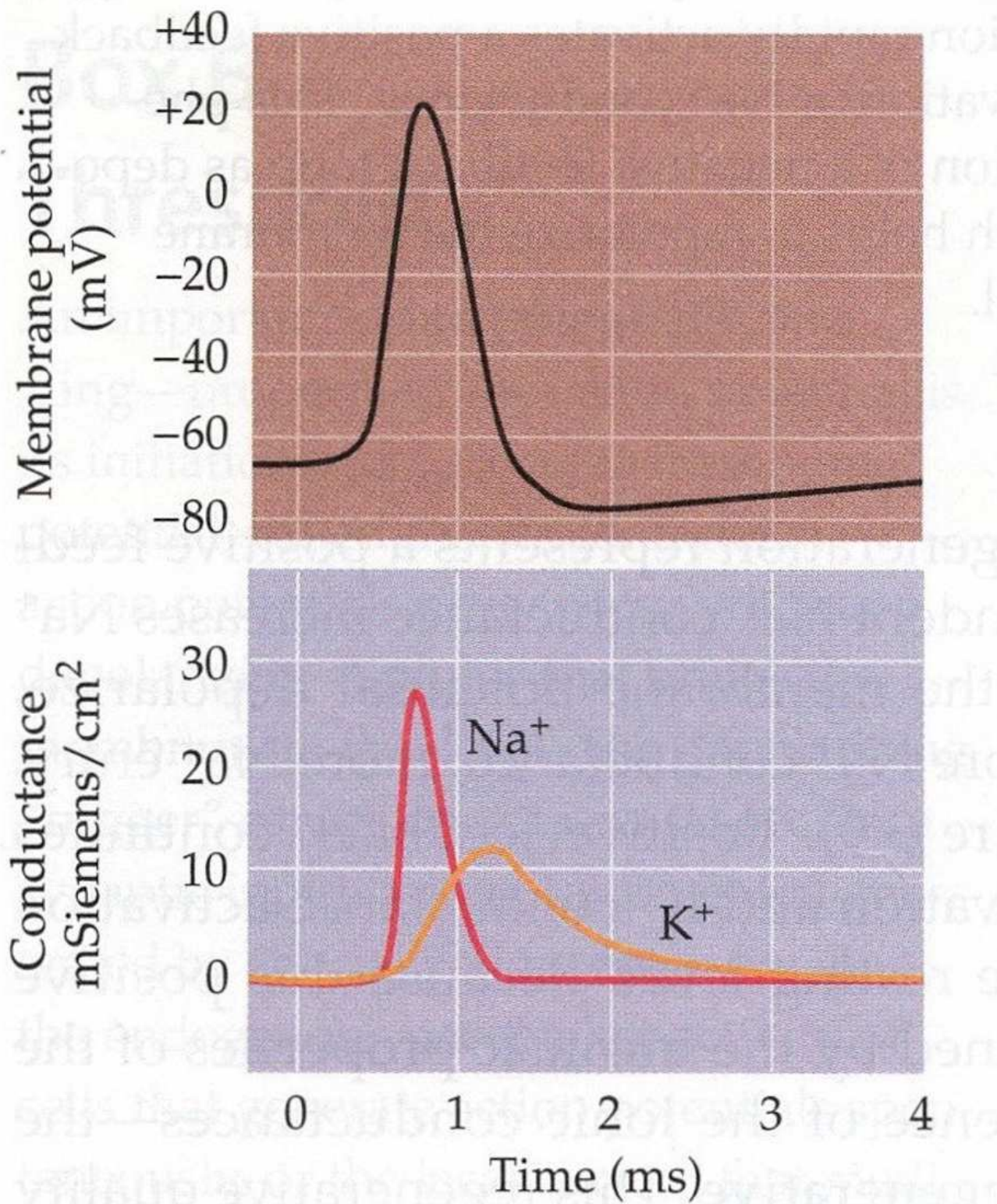


Figure 8

Reconstruction of an action potential after Hodgkin and Huxley, 1952d [4] , courtesy of Purves [6]

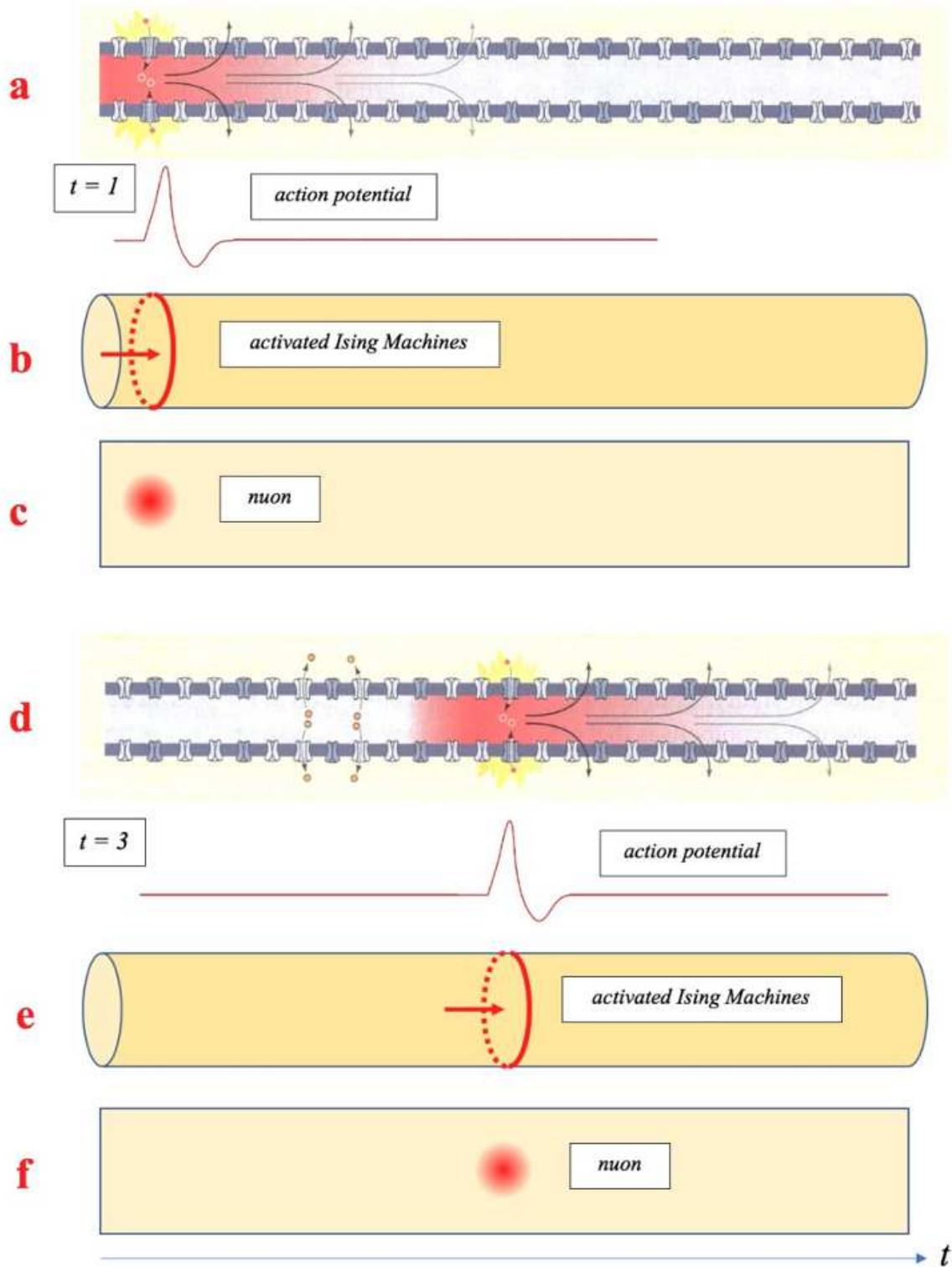


Figure 9

Spikes and nuons. Figures (9a) and (9d) (modified after D. Purves, [6]), show the motion of a spike for $t = 1$ and $t = 3$. Figures (9b) and (9e) show the trigger of a pair of Na^+/K^+ Ising machines housed in annular regions of the membrane for $t = 1$ and $t = 3$. Figures (9c) and (9f) show the motion of a nuon along the axon for $t = 1$ and $t = 3$.

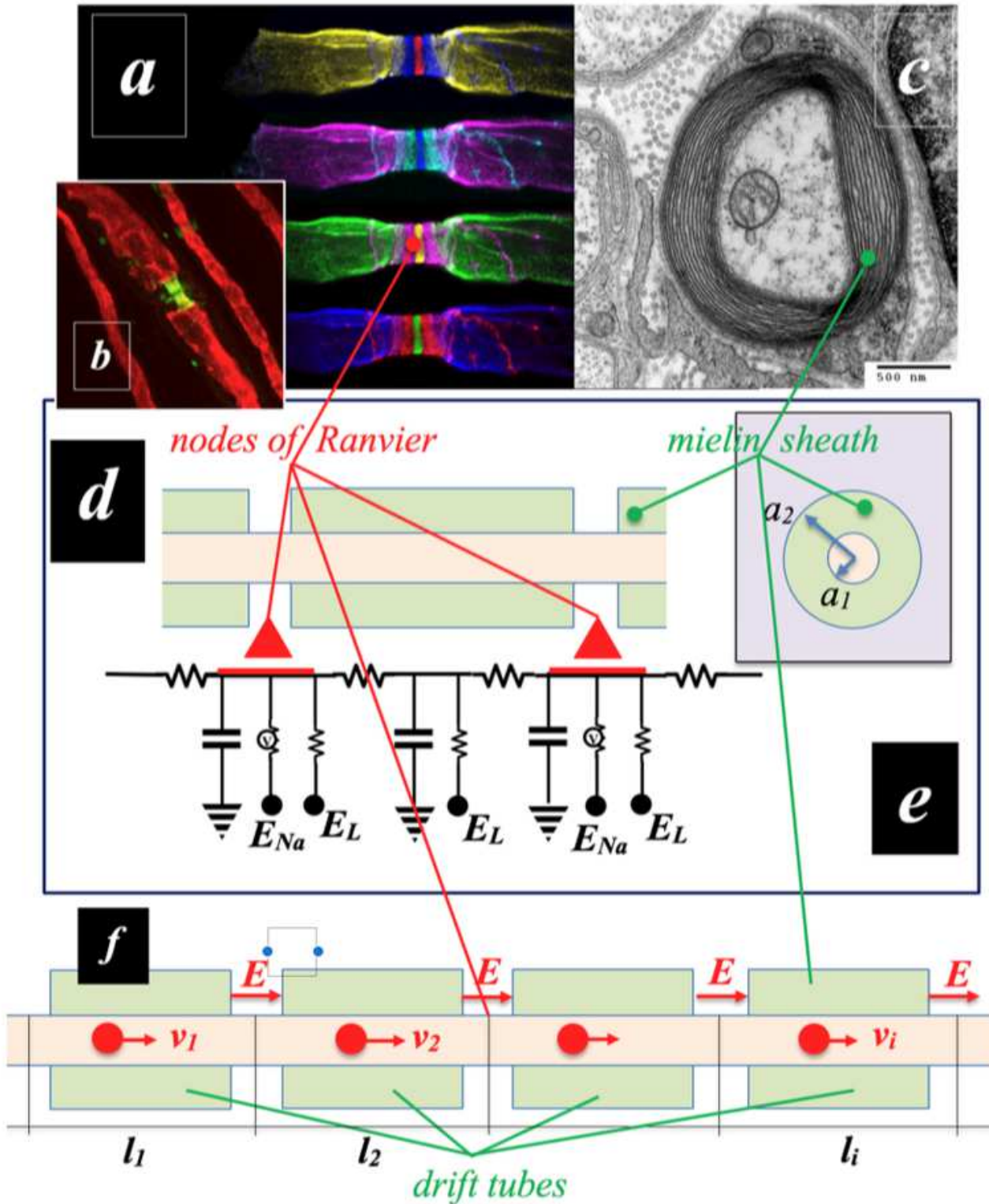


Figure 10

Nodes of Ranvier and Myelin Sheath. Fig. 10a - Courtesy of Anne Desmazieres et Al. [39] . Fig. 10b - Courtesy of Prof. Peter Brophy [46] . Fig. 10c- The structure of the myelin sheath is clearly visible in the electron microscope image. Courtesy by the University of Cambridge, UK. \$. Fig. 10d/e - The nodes of Ranvier and the myelinated regions of an axon are represented as an equivalent circuit within an inter-compartmental model, modified after F. Dayan et al. [8] . Figure 10f - Schematic of our model of a

uLINAC, where an electric field acts in the nodes of Ranvier and accelerates the neurons in the myelinated sections that behave like drift tubes.